MULTI-OBJECTIVE OPTIMIZATION FOR FAULT DETECTION USING A MULTIVARIABLE WAVELET IDENTIFICATION PROCEDURE

Marco Aparecido Queiroz Duarte*, Roberto Kawakami Harrop Galvão†, Henrique Mohallem Paiva‡

*Curso de Matemática, Universidade Estadual de Mato Grosso do Sul - UEMS
Cassilândia, MS, Brasil

†Divisão de Engenharia Eletrônica,Instituto Tecnológico de Aeronáutica - ITA
São José dos Campos, SP, Brasil

‡Mectron - Organização Odebrecht São José dos Campos, SP, Brazil

Emails: marco@uems.br, kawakami@ita.br, hmpaiva@mectron.com.br

Abstract— This paper presents a multi-objective wavelet identification procedure for fault detection in dynamic systems. For this purpose, a multi-objective genetic algorithm is used to search for the Pareto frontier. Two objectives are taken into account, the minimization of the residual signal in nominal operating conditions and its maximization in faulty operating conditions. Thus, the proposed approach takes into account the effect of the fault in the residue. The multivariable consistency check is compared with single variable consistency checks to characterize the advantage of the multivariable approach, providing better fault detection results. For illustration, a simulated example involving the detection of a sensor fault in 747 aircraft is presented.

Keywords— Fault Detection, Pareto Frontier, Dynamic Systems, Wavelets, Multi-objective Optimization.

Resumo— Este artigo apresenta um procedimento multiobjetivo de identificação de parâmetros wavelets para a detecção de falhas em sistemas dinâmicos. Para isto, um algoritmo genético multiobjetivo é usado na busca pela fronteira de Pareto. Dois objetivos são levados em conta, a minimização do sinal residual em condições normais de operação e a sua maximização em condições de falha. Assim, o método proposto leva em consideração o efeito da falha no resíduo. A verificação de consistência multivariável é comparada com a verificação de única variável para mostrar que esta é vantajosa sobre a segunda, levando a melhores resultados na detecção de falhas. Para ilustração, um exemplo simulado envolvendo a detecção de falha em um sensor em uma aeronave 747 é apresentado.

Keywords— Detecção de Falhas, Fronteira de Pareto, Sistemas Dinâmicos, Wavelets, Otimização Multiobjetivo.

1 Introduction

Early detection of fault occurrences is of great importance to the safe operation of dynamic systems, while reducing maintenance costs. Indeed, after the detection of a fault in the system, actions can be taken to avoid damage to the environment, economic losses and loss of human lives. For this purpose time-frequency decomposition techniques, such as the wavelet transform (WT)(Daubechies, 1992), can provide valuable information for the detection process. In fact, the analysis in the frequency domain alone may not reveal faults in their early stages, when the fault signature is not periodic (Paiva et al., 2008).

The WT has been widely applied for fault detection. In (Sartori and Sevegnani, 2010), it was used in a noninvasive methodology to evaluate and classify electrical systems failures. In (Li et al., 2012), bearing faults were detected using a wavelet scheme named adaptive morphological gradient lifting wavelet (AMGLW). The adaptive scheme of AMGLW suppressed the noise present in the signal, emphasizing the fault features. In (Djebala et al., 2012), WT and the Hilbert transform were combined in order to detect and isolate fault in gears. The pairing of these techniques allowed simultaneous filtering and denoising, along with the possibility of detecting transitory phenomena and demodulation. In (Asfani et al., 2012), the WT was used for processing the motor current signal. Energy level of high frequency signal from WT was used as the input for a neural network which worked as a fault detection system. In (Seshadrinath et al., 2012), the dual-tree complex wavelet transform was used to detect single-turn faults in induction motors. In (Paiva et al., 2008), a SISO (single-input, single-output) technique for fault detection was proposed where the WT was directly employed to identify subband models for the normal behavior of the system, which are then used to generate a residual signal. A filter bank implementation of the discrete WT (Daubechies, 1992) was used to band-limit signals acquired at different points of the dynamic system under analysis. A consistency check was then carried out within each of the bands defined by the filter bank. Such a check was performed by comparing the system response with the output of a finite impulse response (FIR) model. In (Paiva et al., 2009), a multivariable extension of (Paiva et al., 2008) was proposed in which several inputs end/or outputs were simultaneously checked for mutual consistency. In that case, the architecture

proposed in (Paiva et al., 2008) was modified to allow the use of MIMO (multiple-input, multiple-output) system identification methods. (Duarte et al., 2013) presented a bi-objective treatment for the cited approach, which consisted in minimizing the residue in nominal operating conditions and maximizing it in fault operating conditions. But, that procedure was made as a linear combination of the two objectives, leading to a mono-objective cost function.

This paper is concerned in giving a multi-objective identification procedure to the fault detection method proposed in (Paiva et al., 2009) and extended in (Duarte et al., 2013). In this paper, the objectives are the same as in (Duarte et al., 2013), but they will be separately treated in order to generate Pareto frontiers for further analysis.

The remainder of this paper is organized as follows. Section 2 presents the necessary background to describe the proposed method and multi-objective optimization process. Section 3 presents the proposed multi-objective optimization procedure. Section 4 describes the application example, which involves the detection of a sensor fault in the simulation of a Boeing 747 aircraft. The results are discussed in Section 5. Finally concluding remarks are presented in Section 6.

2 Background

In (Paiva et al., 2009), which extended the SISO case in (Paiva et al., 2008) to a MIMO case, a multivariable ARX (autoregressive with external input) structure was adopted for each subband model. Fig. 1 shows the scheme proposed in (Paiva et al., 2009) for an input-output scheme, which can be easily extended for an output-output scheme by replacing plant input $\mathbf{u}$ and plant output $\mathbf{y}$ by two plant outputs $\mathbf{y_b}$ and $\mathbf{y_a}$. Filters H and G indicate the low-pass and high-pass filters associated to a particular wavelet, respectively.

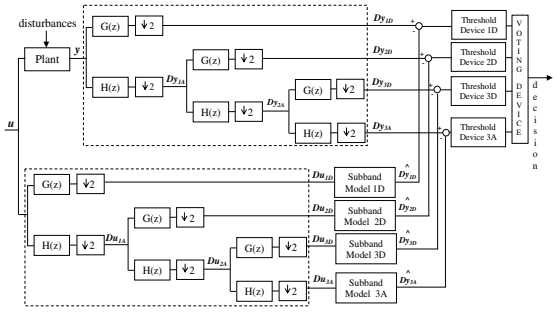

Figure 1: Wavelet-Based Frequency-Subband Analytical Redundancy Scheme. The dashed boxes indicate the wavelet filter bank.

In the wavelet filter bank, the number of filtering iterations leading to a given layer is termed the decomposition level of the layer. In Fig. 1, e.g., the filter bank has three decomposition levels. The best decomposition level for fault detection depends on the spectral signature of the fault, as well as the power spectrum density of the input signal and the signal-to-noise ratio of the measurements (Paiva et al., 2008). If the fault effect has not been previously characterized, all levels should be monitored simultaneously.

The outputs of the low-pass and high-pass filters are termed approximation and detail, respectively. Subscripts iA and iD are used to indicate the approximation and detail at the i-th decomposition level, respectively. The wavelet coefficients $\mathbf{Du}_{i\mathbf{A}}$ (approximation) and $\mathbf{Du}_{i\mathbf{D}}$ (detail) of the input signal $\mathbf{u}$ at the i-th decomposition level, $i > 0$, are calculated as:

$$\mathbf{Du}_{i\mathbf{A}} = (\downarrow 2)[h * \mathbf{Du}_{(i-1)\mathbf{A}}] \tag{1}$$

$$\mathbf{Du}_{i\mathbf{D}} = (\downarrow 2)[g * \mathbf{Du}_{(i-1)\mathbf{A}}] \tag{2}$$

where $(\downarrow 2)$ and $*$ denote the downsampling and convolution operations, and h and g are the discrete-time impulse responses to filters H and G, respectively. The approximation $\mathbf{Du}_{0\mathbf{A}}$ at level 0 is equal to signal $\mathbf{u}$ itself. Similar equations can be used to obtain the wavelet coefficients $\mathbf{Dy}_{i\mathbf{A}}$ (approximation) and $\mathbf{Dy}_{i\mathbf{D}}$ (detail) of the output signal $\mathbf{y}$.

The ARX structure used in (Paiva et al., 2009) is of the form (Ljung, 1999):

$$\hat{\mathbf{Dy}}(k) = \sum_{i=1}^{n_a} A_i \hat{\mathbf{Dy}}(k-i) + \sum_{i=1}^{n_b} B_i \mathbf{Du}(k-i), \quad A_i \in \mathbb{R}^{p\times p}, B_i \in \mathbb{R}^{p\times m} \tag{3}$$

where $\mathbf{Du}(k) \in \mathbb{R}^m$ and $\hat{\mathbf{Dy}}(k) \in \mathbb{R}^p$ correspond to the input and output of the subband model at time index k. Since each subband model is intended to represent the plant behavior only within a limited band, the orders n_a and n_b can be made small. Matrices A_i and B_i can be identified in order to minimize the 2-norm of the difference between the model predictions $\hat{\mathbf{Dy}}$ and the wavelet coefficients $\mathbf{Dy}$ of the actual plant output. For this purpose, a standard multivariable least-squares identification method can be employed (Ljung, 1999).

Both in (Paiva et al., 2008) and (Paiva et al., 2009) a fixed wavelet was used to adjust the parameters of the models in order to minimize the residue between the output of the system and the predicted output. In (Duarte et al., 2013), the concept of wavelet adaptation was exploited to improve the MIMO method proposed in (Paiva et al., 2009). For that purpose, two approaches were considered. The first approach consisted in optimizing the wavelet filter bank parameters to minimize the residue under nominal operating conditions, i.e., to improve the match between the

plant dynamics and the subband model employed in the detector. The second approach also took into account the effects of the fault, by using a bi-objective procedure, minimizing the residue under nominal operating conditions (fault-free) and maximizing it under faulty operating conditions. For both purposes, the wavelet filter bank was parameterized by using a vector of angular parameters $\boldsymbol{\theta} \in \mathbb{R}^n$ as in (Sherlock and Monro, 1988). Those parameters were then optimized in order to minimize the 2-norm of the residue under nominal operating conditions. The bi-objective procedure proposed in (Duarte et al., 2013) was performed by a linear combination of the two objectives cited above. The linear combination permitted a mono-objective treatment to the proposed problem.

The present paper also exploits the concept of wavelet adaptation over the proposal of (Paiva et al., 2009) in a bi-objective way, but using multi-objective optimization algorithms. The wavelet procedure identification will be carried out by using multi-objective genetic algorithms (MOGA), (Konak et al., 2006). The use of MOGA allows the analysis of the Pareto frontier and the choice of the point that leads to more sensibility (fault detection) with low false alarm rate. The advantage of using Pareto frontiers is in the fact that the choice of the point to be analyzed could be made by a selection criterion and this criterion could be changed without the needing of computing the Pareto frontier again.

2.1 Multi-objective Optimization

A multi-objective optimization (MOO) problem has a different perspective when compared with the one having a single objective. In the single-objective optimization there is only one global optimum, but in MOO there is a set of solutions, called Pareto-optimal (PO) set, which are considered to be equally important; all of them constitute global optimum solutions (Bandyopadhyay et al., 2008).

The MOO can be formally stated as follows (Bandyopadhyay et al., 2008). Find the vectors $\bar{x}^* = [x_1^*, x_2^*, ..., x_n^*]^T$ of decision variables that simultaneously optimize the M objective values $\{f_1(\bar{x}), f_2(\bar{x}), ..., f_M(\bar{x})\}$, while satisfying the constraints, if any.

The concept of domination is very important in MOO. In the context of a minimization problem, a solution $\bar{x}_i$ is said to dominate $\bar{x}_j$ if $\forall k \in 1, 2, ..., M$, $f_k(\bar{x}_i) \leq f_k(\bar{x}_j)$ and $\exists k \in 1, 2, ..., M$, such that $f_k(\bar{x}_i) < f_k(\bar{x}_j)$.

Among the set of solutions P, the nondominated set of solutions P' are those that are not dominated by any member of the set P. The nondominated set of the entire search space S is the globally PO set. In general, a MOO algorithm usually admits a set of solutions that are not dominated by any solution encountered by it.

3 Proposed Method

Let $A = (A_1, A_2, ..., A_{na})$ and $B = (B_1, B_2, ..., B_{nb})$ be the matrices of the ARX model (3) at a certain subband. Given the data set $\boldsymbol{\mathcal{D}^N} = (\boldsymbol{u^N}, \boldsymbol{y^N})$ of input/output signals acquired under nominal conditions and a wavelet filter bank described by a parameter vector $\boldsymbol{\theta} \in \mathbb{R}^n$, the model matrices A and B can be identified by minimizing a cost function corresponding to the 2-norm of the vector of residues $\boldsymbol{e_D} = (\boldsymbol{Dy} - \boldsymbol{\hat{D}y})$. In view of the dependence of the resulting matrices with respect to the data set and the filter bank, the cost function will be denoted as

$$J^N(A, B, \boldsymbol{\theta}; \boldsymbol{\mathcal{D}^N}) = \frac{1}{2}\boldsymbol{e_D}\boldsymbol{e_D^T}, \tag{4}$$

where superscript N is employed to indicate nominal operating conditions. The identification result will be written as $A^N(\boldsymbol{\theta})$, $B^N(\boldsymbol{\theta})$, where

$$(A^N(\boldsymbol{\theta}), B^N(\boldsymbol{\theta})) = \underset{A \in \mathbb{R}^{p \times p}, B \in \mathbb{R}^{p \times m}}{\arg\min} J^N(A, B, \boldsymbol{\theta}; \boldsymbol{\mathcal{D}^N}). \tag{5}$$

When the objective is to minimize the residue under nominal operating conditions using the wavelet adaptation, a vector $\boldsymbol{\theta}_N^*$ is found in order to minimize a cost function $\tilde{J}^N(\boldsymbol{\theta})$ so that

$$\tilde{J}^N(\boldsymbol{\theta}_N^*) = \min_{\boldsymbol{\theta} \in \mathbb{R}^n} J^N(A^N(\boldsymbol{\theta}), B^N(\boldsymbol{\theta}), \boldsymbol{\theta}; \boldsymbol{\mathcal{D}^N}). \tag{6}$$

On the other hand, in order to increase the detector sensitivity with respect to the fault, it may be convenient to adjust $\boldsymbol{\theta}$ to maximize the residue under faulty conditions, i.e., to maximize a cost function $\tilde{J}^F(\boldsymbol{\theta})$ so that

$$\tilde{J}^F(\boldsymbol{\theta}_F^*) = \max_{\boldsymbol{\theta} \in \mathbb{R}^n} J^F(A^N(\boldsymbol{\theta}), B^N(\boldsymbol{\theta}), \boldsymbol{\theta}; \boldsymbol{\mathcal{D}^F}), \tag{7}$$

where the superscript F indicates faulty operating conditions.

In order to aggregate (6) and (7), i.e., to achieve a compromise between minimizing the residue under nominal operating conditions and maximizing it under faulty conditions, the following bi-objective cost function should be minimized

$$\tilde{J}^{NF}(\boldsymbol{\theta}_{NF}^*) = \min_{\boldsymbol{\theta} \in \mathbb{R}^n} [J^N(\boldsymbol{\theta}), -J^F(\boldsymbol{\theta})]. \tag{8}$$

For a better graphical visualization of the plots of $J^N \times J^F$, (8) can be written in terms of $log_{10}(J^N(\boldsymbol{\theta}))$ and $log_{10}(J^F(\boldsymbol{\theta}))$, leading to (9).

$$\tilde{J}^{NF}(\boldsymbol{\theta}_{NF}^*) = \min_{\boldsymbol{\theta} \in \mathbb{R}^n} [log_{10}(J^N(\boldsymbol{\theta})), -log_{10}(J^F(\boldsymbol{\theta}))]. \tag{9}$$

In this paper, (9) will be adopted.

It is worth noting that the formulation presented here is the same presented in (Duarte

et al., 2013). But now, differently from the proposal of (Duarte et al., 2013) the wavelet identification procedure takes place directly using (9), instead of a linear combination of the two objectives in (8). This approach enables the choice of a point in the Pareto frontier, the one that best matches better sensibility and low false alarm rates.

4 Application Example

In order to test the proposed method, a simulation model of the lateral dynamics of a Boeing 747 aircraft in landing configuration (Bryson, 1985) was used. This simulation model can be written as

$$\begin{bmatrix}\dot{v}\\ \dot{r}\\ \dot{p}\\ \dot{\phi}\end{bmatrix} = \begin{bmatrix}-0.089 & -2.19 & 0.328 & 0.319\\ 0.076 & -0.217 & -0.166 & 0\\ -0.602 & 0.327 & -0.975 & 0\\ 0 & 0.150 & 1 & 0\end{bmatrix}\begin{bmatrix}v\\ r\\ p\\ \phi\end{bmatrix} + \begin{bmatrix}0 & 0.0327\\ 0.0264 & -0.151\\ 0.227 & 0.0636\\ 0 & 0\end{bmatrix}\begin{bmatrix}\delta a\\ \delta r\end{bmatrix} + \begin{bmatrix}0.089\\ -0.076\\ 0.602\\ 0\end{bmatrix} d \tag{10}$$

where v is the sideslip velocity, r is the yaw rate, p is the roll rate, ϕ is the roll angle, δa is the aileron angle, δr is the rudder angle, and d is an exogenous disturbance (lateral wind velocity). The adopted units are feet, seconds, and crad (0.01 rad). The system is operated under a control law of the form

$$\begin{bmatrix}\delta a\\ \delta r\end{bmatrix} = -\begin{bmatrix}-4.15 & 7.6 & 5.36 & 5.57\\ 3.43 & -14.24 & 0.62 & -0.24\end{bmatrix}\begin{bmatrix}v\\ r\\ p\\ \phi\end{bmatrix} \tag{11}$$

which places the closed-loop poles at -2, -1 and $-1 \pm 2j$ (Paiva et al., 2008). Each measured state is assumed to be corrupted by an additive white noise with a standard deviation equal to 2% of the standard deviation of the true signal. The disturbance d was generated as a low-pass-filtered Gaussian noise with a standard deviation of 10 ft/s.

The problem consists of detecting a gain reduction in the rate gyro responsible for measuring the yaw rate r. Fig. 2 presents an example of a fault at $t_f = 100$ s. Training and test signals were acquired with a sampling frequency $f_s = 100$ Hz.

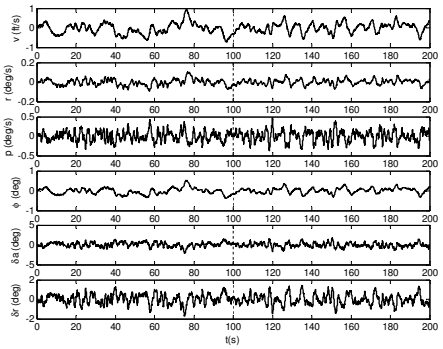

Figure 2: Simulation of the 747 aircraft model with a fault at $t_f = 100$ s (angles in degrees).

5 Fault Detection Results

In order to apply the proposed fault detection method, the db8 wavelet filters (Daubechies, 1992) were used as a starting point for the optimization procedure. The choice for these filters was based on the results presented in (Paiva et al., 2008), (Paiva et al., 2009) and (Duarte et al., 2013). The optimization process for MOGA was carried out by a MATLAB implementation as in the MATLAB® Global Optimization Toolbox.

In this work, the detection threshold was fixed as four times the standard deviation of the residue in nominal operating conditions. For fault detection, as in (Paiva et al., 2009), the overall fault monitor, in Fig. 1, declared a fault if any threshold detector was activated.

In the aircraft simulation, the proposed wavelet method was applied to check the consistency between sensors using SISO and MIMO approaches. For the SISO approach, consistencies between sensors (p, r) and (ϕ, r) were checked. In those cases, in Fig. 1, $\mathbf{y} = r$ and $\mathbf{u} = p$ or $\mathbf{u} = \phi$. For the MIMO approach, consistency between sensors (p, ϕ) and r was checked. Now, in Fig. 1, $\mathbf{u} = [p\ \phi]^T$ and $\mathbf{y} = r$. Three wavelet decomposition levels were used in the wavelet filter banks. The ARX orders were the same adopted in (Paiva et al., 2009) for each subband model, namely which will be $n_a = 1$ and $n_b = 2$. For the three consistency checks, Pareto frontiers were generated for each wavelet decomposition level.

Fig. 3 shows the Pareto frontiers for the three consistency checks. Observing Fig. 3, it is possible to note that, in each wavelet decomposition level, the point that best comprises the minimization of J^N and the maximization of J^F is the one that maximizes the distance of the green diagonal line. The choice for this point provides $J^N << J^F$, which is desired for appropriated fault detections. In this context, it is worth noting that, for each wavelet decomposition level, the multivariable approach has the best point, while (ϕ, r) has the worst. It is also worth noting that the solutions of the Pareto frontier of (p, ϕ, r) are never dominated by the solutions in the Pareto frontiers of (p, r) or (ϕ, r), but they dominate almost all of the points of (p, r) or (ϕ, r).

In (Paiva et al., 2009) the db8 wavelet filters (Daubechies, 1992) were used as a fixed wavelet in the identification procedure for the ARX model. Fig. 4 presents the Pareto frontiers of (p, ϕ, r) and the point for the fixed db8 filters, also for (p, ϕ, r), for three wavelet decomposition levels. In Fig. 4, it is possible to observe the advantage of the use of MOO in the wavelet identification process, since the point representing the fixed db8 filters is very close to diagonal line, in each wavelet decomposition level.

Further tests for fault detection were carried

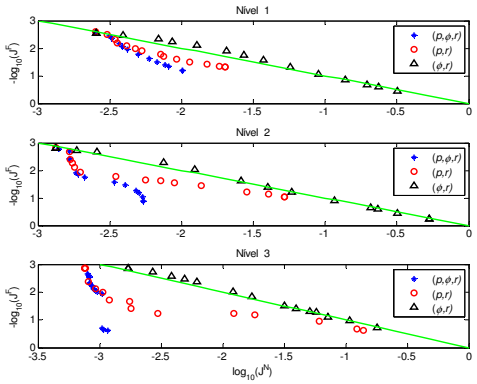

Figure 3: Pareto frontiers for the three consistency checks, for three wavelet decomposition levels.

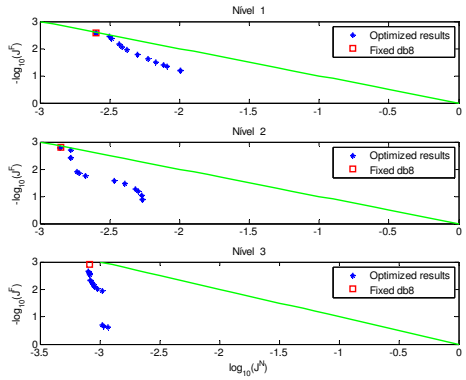

Figure 4: Pareto frontiers for multi-objective (p, ϕ, r), and the points for the fixed db8 filters, for three wavelet decomposition levels.

out by choosing a point for each consistency check in each Pareto frontier in Fig. 3 for the three wavelet decomposition levels, according to the observation made in the last paragraph, i.e., the one that maximizes the distance from the diagonal line in the graph. For tests, a gain reduction of 30% in the rate gyro was adopted, and 11 realizations were performed with different seed values for the noisy disturbance. Data for the obtainment of the Pareto frontiers and for the identification procedure were carried out for a 50% gain reduction in the rate gyro.

In order to clarify the advantage of one methodology over the others, the following metric Γ was evaluated (Paiva et al., 2008):

$$\Gamma = \frac{\max(\text{abs}(\text{residue}_{\text{after}-\text{fault}}))}{\max(\text{abs}(\text{residue}_{\text{before}-\text{fault}}))} \qquad (12)$$

which characterizes the residue amplification after fault occurrence. Large values of Γ are desired because they allow the use of a larger residue threshold in the fault detection scheme, thus minimizing the probability of false alarms.

For illustration, Fig. 5 shows the residues obtained using the three consistency checks for a particular fault simulation. In Fig. 5 the horizontal dashed lines indicate the threshold for fault detection, the vertical dashed lines indicate the fault onset at t = 100 s, t_d is the detection delay, defined as the difference between the instant when the residue exceeded the threshold and the instant when the fault occurred, and Γ indicates the residue amplification according to (12).

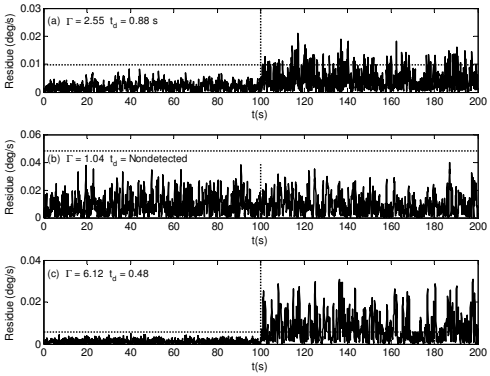

Figure 5: Subband residues for details, at the third wavelet decomposition level, obtained by processing signals depicted in Fig. 2 with consistency checks (a) (p, r), (b)(ϕ, r), and (c) (p, ϕ, r).

Table 1 presents Γ values (average and standard deviation) obtained applying the points chosen in the Pareto frontier, for three wavelet decomposition levels of the consistency checks. Comparing Γ values presented in Table 1, it is easy to note that the multivariable approach is advantageous over the single variable approaches, leading to the largest values of Γ. Mainly, for the third wavelet decomposition level, where the multivariable value for Γ was much larger than the ones for the single variable approaches.

Table 2 shows, for the third wavelet decomposition level, the average detection delay t_d and its standard deviation (out of eleven simulations) for each consistency check, when a 30% gain reduction in the rate gyro was performed. For the three consistency checks, no false alarm was issued. The mean value for t_d was calculated by considering only the successful detections, i.e., by ignoring false alarms and nondetected faults. As can be seen, again, multivariable approach was better than the other two approaches, leading to smaller detection delays. This shows that a fault could be detected faster when two or more sensors are used for consistency check with the sensor containing the fault.

The results presented in Tables 1 and 2 and in Fig. 5 showed that the consistency check (p, ϕ, r) provided a better estimate of the output r than when only p or ϕ were used to check consistency with r.

6 Conclusion

This paper extended a recent wavelet-based multivariable fault detection method to a multi-objective optimization formulation for the wavelet identification procedure. The multi-objective pro-

Table 1: Comparison Between Mean Values of Γ (eleven simulations) obtained for different wavelet decomposition levels, for a 30% gain reduction in the rate gyro.

Level	(p, r)	(ϕ, r)	(p, ϕ, r)
1	1.73 ± 0.06	1.18 ± 0.03	1.92 ± 0.03
2	2.48 ± 0.10	1.63 ± 0.06	2.85 ± 0.08
3	2.73 ± 0.05	0.93 ± 0.01	6.63 ± 0.06

Table 2: Mean detection delay, t_d, for the three consistency checks, at the third wavelet decomposition level, for a 30% gain reduction in rate gyro.

Approach	$t_d(s)$
(p, r)	1.3 ± 0.11
(ϕ, r)	Nondetected
(p, ϕ, r)	0.45 ± 0.01

cedure consisted in minimizing the residue in nominal operating conditions and maximizing it in faulty operating conditions. Besides the multi-objective formulation, comparisons between multivariable and the single variable consistency checks were also subject in this paper. Fault detection was carried out by checking the mutual consistency of two or three different sensor signals of a simulation of the lateral dynamics of a Boeing 747 aircraft in landing configuration. In order to show that the multivariable consistency check is advantageous over the single variable one, using multi-objective genetic algorithms, Pareto frontiers were obtained, showing that the multivariable provides points in the Pareto frontier that conduces to better results than the single variable approach. Choosing a point for each Pareto frontier, it was shown that the multivariable consistency check provided better results than the others, since faults were detected for all wavelet decomposition levels in less time with no false alarm occurred. Analyzing the residues in nominal and fault operating conditions, it was shown improvement in sensitivity of the multivariable approach with respect the single variable approach. This was due to fact that for multivariable approach the residue amplification after the fault occurrence was much larger than for the single variable approach.

Acknowledgments

This work was supported by CNPq (research fellowships and post-doctoral grant 150213/2012-3) and FAPESP (grant 2011/17610-0).

References

Asfani, D. A., Muhammad, A. K., Syafaruddin, Purnomo, M. H. and Hiyama, T. (2012). Temporary short circuit detection in induction motor winding using combination of wavelet transform and neural network, *Expert Systems with Applications* **39**(5): 5367–5375.

Bandyopadhyay, S., Saha, S., Maulik, U. and Deb, K. (2008). A simulated annealing-based multiobjective optimization algorithm: AMOSA, *IEEE Trans. on Evolutionary Computation* **12**(3): 269–283.

Bryson, A. E. (1985). New concepts in control theory, *J. of Guid. Control and Dynamics* **8**(4): 1959–1984.

Daubechies, I. (1992). *Ten Lectures on Wavelets*, SIAM.

Djebala, A., Ouelaa, N., Benchaabane, C. and Laefer, D. F. (2012). Application of the wavelet multi-resolution analysis and Hilbert transform for the prediction of gear tooth defects, *Meccanica* **47**(7): 1601–1612.

Duarte, M. A. Q., Galvão, R. K. H. and Paiva, H. M. (2013). Bi-objective optimization in a wavelet identification procedure for fault detection in dynamic systems, In: *The IEEE 8th Conference on Industrial Electronics and Applications (ICIEA)*, v. 1, p. 1319–1324, Melbourne, Australia, 19-21 June.

Konak, A., Coit, D. W. and Smith, A. E. (2006). Multi-objective optimization using genetic algorithms: A tutorial, *Reliability Eng. and System Safety* **91**(9): 992–1007.

Li, B., lin Zhang, P., shan Mi, S., xi Hu, R. and sheng Liu, D. (2012). An adaptive morphological gradient lifting wavelet for detecting bearing defects, *Mech. Syst. and Signal Process.* **29**: 415–427.

Ljung, L. (1999). *System Identification: Theory for the User*, 2nd edn, Prentice Hall.

Paiva, H. M., Galvão, R. K. H. and Rodrigues, L. (2009). A wavelet-based multivariable approach for fault detection in dynamic systems, *Controle & Automação* **20**(4): 455–464.

Paiva, H. M., Galvão, R. K. H. and Yoneyama, T. (2008). A wavelet band-limiting filter approach for fault detection in dynamic systems, *IEEE Trans. on Syst., Man, and Cybernetics - Part A: Systems and Humans* **38**(3): 681–687.

Sartori, C. A. F. and Sevegnani, F. X. (2010). Fault classification and detection by wavelet-based magnetic signature recognition, *IEEE Trans. on Magnetics* **46**(8): 2880–2883.

Seshadrinath, J., Singh, B. and Panigrahi, B. K. (2012). Single-turn fault detection in induction machine using complex-wavelet-based method, *IEEE Trans. on Ind. App.* **48**(6): 1846–1854.

Sherlock, B. G. and Monro, D. M. (1988). On the space of orthonormal wavelets, *IEEE Trans. Signal Process* **46**(6): 1716–1720.